

Inhalable Chitosan Tripolyphosphate Nanoparticles for Extended Release of DTPA into Lung Fluid

Chen S¹, Lai EPC^{1*}, Ko R², Li CS² and Wyatt H³

¹Department of Chemistry, Carleton University, Canada

²Radiation Protection Bureau, Health Canada, Canada

³Canadian Nuclear Laboratory, Chalk River, Canada

***Corresponding author:** Edward PC Lai, Department of Chemistry, Carleton University, 1124 Colonel By Drive, Ottawa, ON K1S 5B6, Canada, Tel: (613) 520-2600-3835; E-mail: edward.lai@carleton.ca

Research Article

Volume 1 Issue 1

Received Date: September 18, 2016

Published Date: October 14, 2016

DOI: 10.23880/nnoa-16000106

Abstract

Diethylenetriaminepentaacetic acid (DTPA) is a non-toxic chemical agent with strong actinide chelation properties that has been approved for decorporation of internalized radioactive nuclides such as plutonium and americium. However, DTPA exhibits poor inhalation delivery efficacy for emergency treatment due to short retention in the lungs. Chitosan (CS) is a biodegradable, biocompatible and hydrophilic polymer that adheres to biological mucosa. CS nanoparticles encapsulating DTPA were prepared by the ionic gelation method using sodium tripolyphosphate (TPP). The CS-DTPA/TPP nanoparticles have been characterized for reversible unfolding in a simulated lung fluid. Extended release of the agent, for improved efficacy of actinide decorporation, was monitored by liquid chromatography-mass spectrometry. The *in vitro* release profile exhibits an initial burst, followed by a sustained release to reach finally a stable level. More importantly lysozyme, a protein in respiratory tract secretions, exhibits no negative impact on the extended release of DTPA from the CS-DTPA/TPP nanoparticles.

Keywords: Chitosan; Decorporation agent; DTPA; Ionic gelation; Simulated lung fluid; Nanoparticles; *In vitro* release

Introduction

Nuclear energy is considered as a clean and cost-effective power resource that has gained world-wide popularity over the past 5 decades. However globally there have been recorded nuclear accidents (that either resulted in the loss of human life or more than US\$50,000 of property damage), including ten accidents in Canada from 1952 to 2011 [1]. Radionuclides can be released into the environment during nuclear accidents, such as the reactors at Chernobyl [2] and Fukushima [3], with the

potential to pose risks to human health through external exposure or internal contamination (inhalation, ingestion or wound). Internalized radionuclides can be transported by the blood and deposit in the target organs such as bones, kidneys and liver [4]. Effective treatments vary for different radionuclides and are related to intake pathways, the level of contamination, the chemical form of each radionuclide, as well as the time interval between contamination and treatments [5-7]. For internal

contamination with actinides such as plutonium and americium, timely administration of decorporation agents is crucial for effective treatment. The U.S. Project BioShield Act of 2004 authorized the Department of Health and Human Services (DHHS) to treat, identify or prevent harm from any biological, chemical, radiological, or nuclear agent that may cause a public health emergency affecting national security [8]. Consistent with this authority, the National Institute of Allergy and Infectious Diseases (NIAID) focused on the development of novel radionuclide chelation and decorporation agents. These agents chelate with actinides and form soluble stable complexes that can be excreted from the body.

Diethylenetriaminepentaacetic acid (DTPA) is an effective decorporation agent to remove tetravalent actinides [9]. It is currently still the only commercially available chelating drug that can be used for decorporation of internalized plutonium and americium [10]. Pu DTPA⁻ and Pu(OH)DTPA²⁻ are the two stable species of plutonium present in blood [11]. Injectable formulations of DTPA have been approved by the FDA, and a diethyl ester prodrug of DTPA is being investigated as an oral decorporation agent [12]. Calcium and zinc diethylenetriaminepentaacetates (Ca-DTPA and Zn-DTPA) are the most common forms used for radionuclide decorporation. Ca-DTPA chelates transuranic metals (americium, californium, curium, neptunium, plutonium), rare earth metals (cerium, lanthanum, yttrium) and transition metals (niobium, zirconium) [13]. Zn-DTPA is regarded as an effective decorporation agent for the treatment of internal contamination by Pu and Am with less toxic effect than Ca-DTPA [14]. These two pentaacetate salts are most effective if the actinides to be chelated are in soluble forms [15]. However, as more than 90% of the administered DTPA is excreted within 24 hours, repeated doses are often necessary to achieve the required decorporation efficacy [16]. Direct lung delivery of the chelating agent to the alveolar region may increase its local concentration as compared to systemic delivery and therefore increase the extent of decorporation [17].

Chitosan, a linear polymer of β -linked 2-amino-2-deoxy-D-glucose residues, is a deacetylated form of chitin, the most abundant natural polymer after cellulose. Chitosan can be prepared from chitin (poly β -(1 \rightarrow 4)-N-acetyl-D-glucosamine) by chemical N-deacetylation up to 50% [18,19]. Chitosan is a non-toxic, biodegradable and biocompatible polymer. It shows biological, physiological and pharmacological properties that are different from

cellulose. These biological properties include antimicrobial activity, eliciting biological responses, mucoadhesion, hypolipidemic activity, immune enhancement, hemostatic activity, and promotion of wound healing [18]. Chitosan has been proposed to be applied in mucosal drug delivery owing to its mucoadhesion activity [20]. It has been used as a drug carrier for peptide drugs in the nasal and peroral delivery, in order to improve drug absorption [21,22]. The cationic polyelectrolyte property of chitosan allows interaction with a negatively charged mucosal surface [23].

Lysozyme existing in serum can degrade chitosan [24]. The degree of N-deacetylation and molecular weight of chitosan can affect lysozyme degradation behavior [25]. The degradation process is very slow for the chitosan with a relatively high deacetylation degree while those with a low deacetylation degree experience faster degradation process [26]. The chitosan with lower molecular weight will be degraded faster in lysozyme than the chitosan with higher molecular weight [25]. The *in vitro* lysozyme degradation under the physiological conditions (pH=7.4, 37°C) indicates that the cumulative mass loss reaches approximately 46% for the porous Chitosan (deacetylation degree= 89%) membrane after 7 days [25].

The purpose of this work was to combine the biochemical properties of chitosan and DTPA to improve the efficacy of decorporation therapy. Ionic gelation method was applied in preparing chitosan nanoparticles with encapsulated DTPA, using sodium tripolyphosphate (TPP) as a cross-linker. The synthesized CS-DTPA/TPP nanoparticles were characterized by several instrumental analysis techniques. *In vitro* release was studied to determine the release profile of CS-DTPA/TPP nanoparticles. Lysozyme was assessed for its effect on the DTPA release behavior due to degradation of chitosan.

Materials and Methods

Materials

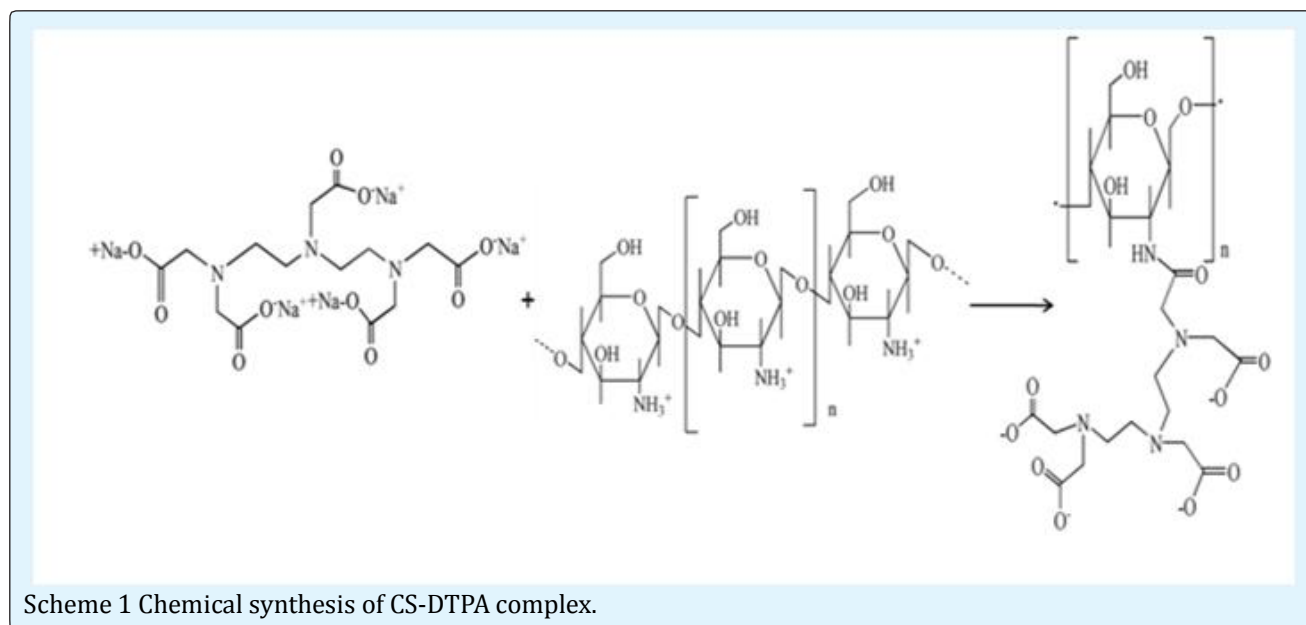
Chitosan (low molecular weight), diethylenetriaminepentaacetic acid pentasodium salt solution (40% in H₂O), D-mannitol (Bioultra \geq 99.0%), formic acid, iron(III) chloride hexahydrate, magnesium chloride hexahydrate, sodium acetate, sodium hydroxide, sodium tripolyphosphate pentabasic, and lysozyme (from chicken egg white, lyophilized powder, protein \geq 90%, \geq 40,000 units/mg protein) were purchased from Sigma-Aldrich. Acetic acid (glacial) was purchased from EMD

Chemicals. Regenerated cellulose dialysis membranes (MWCO 3500) were purchased from Thermo Fisher Scientific.

Preparation of CS-DTPA complex

The CS-DTPA complex was synthesized according to a previously reported method [27]. First, chitosan was dissolved in 1% acetic acid in order to obtain positively

charged chitosan at the concentration of 1mg/mL. Next, 40% DTPA-Na salt solution was added into the chitosan-acetic acid solution at different weight ratios between DTPA and chitosan. Negatively charged DTPA was allowed to react with positively charged chitosan overnight to form the CS-DTPA complex, following the equation in Scheme 1.



Preparation of CS-DTPA/TPP nanoparticles

Nanoparticles were prepared from the CS-DTPA complex solution by the ionic gelation method, a reversible physical cross-linking process that relies on electrostatic attraction instead of chemical bonds [28]. The CS-DTPA complex solution was adjusted to pH 4.5 using 2 M NaOH solution. An aqueous solution of sodium TPP was prepared at a concentration of 0.5mg/mL. Under mild magnetic stirring at room temperature, the TPP solution was added drop wise to the CS-DTPA complex solution to attain different CS/TPP weight ratios. The mixture was stirred continuously for 1 hour to form CS-DTPA/TPP nanoparticles in aqueous suspension.

Preparation of CS-DTPA/TPP dry powders

Freezing drying was used to prepare CS-DTPA/TPP dry powders from the above suspension. An aqueous solution of 5% mannitol was prepared to act as dispersant that prevented the aggregation of CS-DTPA/TPP nanoparticles during the freeze drying process. The aqueous suspension

of CS-DTPA/TPP nanoparticles was added into the mannitol solution. The final CS-DTPA/TPP mannitol complex was pre-frozen overnight. Dry powders of CS-DTPA/TPP/mannitol were finally obtained in a Labconco model 7753020 freeze dryer operating at a temperature of -53°C.

Characterization of nanoparticles by transmission electron microscopy

Transmission electron microscopy (TEM) was used to characterize the CS-DTPA/TPP nanoparticles on a FEI Tecnai G2 F20 microscope operating at 200 kV. The TEM analysis offered a point resolution of 0.27 nm and a magnification ranging from 21x to 700,000x.

Characterization of nanoparticles by Fourier transform infrared spectroscopy

The molecular structure of CS-DTPA/TPP dry powders (with different weight ratios of chitosan to DTPA) were characterized using an ABB Bomem MB Series Fourier

transform infrared (FTIR) spectrometer. Disc samples were prepared by grinding and compressing a small amount of sample (~2mg) with spectro photometric-grade KBr (~200 mg). All FTIR spectra were obtained in the spectral region of 600-4000 cm^{-1} .

Characterization of nanoparticles by dynamic light scattering

Dynamic light scattering (DLS) was used to measure the hydrodynamic size distribution of CS-DTPA/TPP/mannitol dry powders dispersed in a buffer solution that was prepared by dissolving 1mmol of sodium acetate in 1% (v/v) acetic acid solution. Each dispersion was ultra-sonicated for 5 minutes before DLS analysis using a Brookhaven Instruments nano DLS particle size analyzer (Holtsville, NY, USA). Ten replicate measurements of 10 s each were performed to ensure high accuracy.

In vitro release of DTPA from CS-DTPA/TPP nanoparticles

Gamble's solution was prepared as the simulated lung fluid (SLF) with pH 7.4 for *in vitro* release tests because it represents the interstitial fluid deep inside the lungs down to the alveoli [29]. The CS-DTPA/TPP/mannitol dry powders were dissolved in the SLF at a concentration of 10mg/mL. Lysozyme could be added to reach a concentration of 10 mg/mL. The suspension of recovered CS-DTPA/TPP nanoparticles in SLF was placed in a dialysis tube. The dialysis tube was then immersed to a beaker of 50mL SLF kept at $37 \pm 1^\circ\text{C}$ under stirring. At appropriate time intervals, a sample of dialysate was withdrawn. Meanwhile, an equal volume of fresh SLF was added in the dialysis beaker to keep the volume of SLF constant. The release test was continued for seven days and the last dialysate sample was collected at 168 hours after the beginning.

Determination of DTPA concentration by liquid chromatography-tandem mass spectrometry

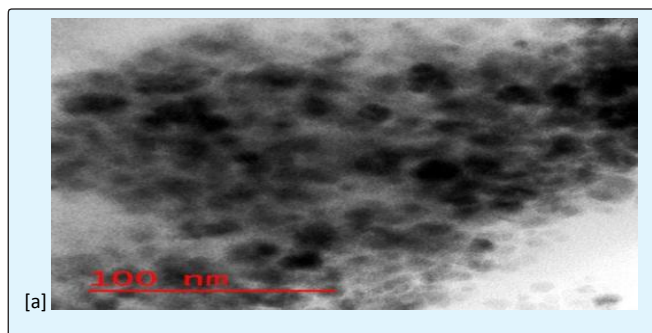
The dialysate samples collected from the release tests (in the absence and presence of lysozyme) were analyzed by liquid chromatography-tandem mass spectrometry (LC-MS/MS) to determine their DTPA concentrations. Fe(III) ions were added into all DTPA standard solutions and dialysate samples; DTPA chelated with Fe(III) ions to form stable $[\text{M} - 4\text{H}^+ + \text{Fe}^{3+}]^-$ cluster ions. All Fe(III)-DTPA standards and dialysate samples were diluted with 0.1% formic acid before the analysis. LC was carried out on aC18 column (50mm x 2.1mm) maintained at room

temperature using two solvents: 0.1% formic acid in ultrapure water (A) and 0.1% formic acid in acetonitrile (B). The mobile phase was prepared by mixing 98% A and 2% B. Formic acid could increase the electrospray ionization (ESI) sensitivity by forming protonated ions. The flow rate was set at 0.400mL/min. Mass spectrometry analysis was performed using an Agilent Technologies model 6460 triple quad MS/MS system which was equipped with an ESI source operating in the negative mode. The operating parameters were: gas flow rate = 9.8 L/min, gas temperature = 300°C , nebulizer pressure = 15 psi, capillary voltage = 4000V, fragment or voltage = 135V, and cell accelerator voltage = 7V. Single ion monitoring was set up to record the peak at $m/z = 445$.

Results and Discussion

Characterization of morphology, size distribution and molecular structure

The CS-DTPA/TPP nanoparticles, synthesized by ionic gelation of CS-DTPA with TPP, were characterized by several instrumental methods to determine their morphology, size distribution and molecular structure. First, TEM was used to examine CS-DTPA/TPP nanoparticles with two different chitosan to DTPA weight ratios. (Figure 1a) shows the spherical morphology of CS-DTPA/TPP nanoparticles prepared using a chitosan to DTPA weight ratio of 1:2.5. The irregularly shaped morphology of CS-DTPA/TPP nanoparticles prepared using a chitosan to DTPA weight ratio of 1:25 can be observed in (Figure 1b). Obviously these TEM images show that the synthetic CS-DTPA/TPP nanoparticles are all smaller than 50 nm, which is good for their nasal administration down to the lower respiratory tract in human lungs. Aggregation of nanoparticles, albeit inevitable in the dried sample for TEM analysis, may not be detrimental to the efficacy of decorporation therapy as DTPA can be released from the nanoparticles after delivery by a jet nebulizer for aerosol deposition into lung fluid.



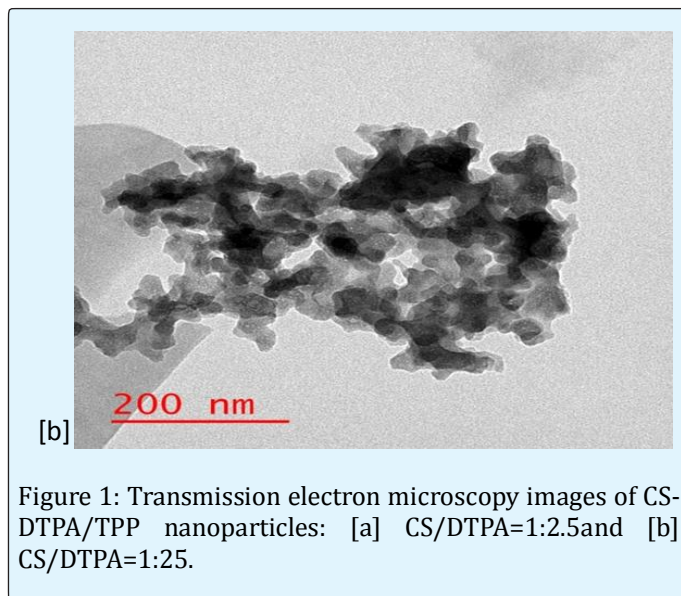


Figure 1: Transmission electron microscopy images of CS-DTPA/TPP nanoparticles: [a] CS/DTPA=1:2.5 and [b] CS/DTPA=1:25.

Next, the hydrodynamic diameter of CS-DTPA/TPP nanoparticles was analyzed by DLS. (Figure 2a) presents the size distribution of nanoparticles synthesized with a chitosan to DTPA weight ratio of 1:1. Most particles (72%) are in the size range of 0-50 nm while some particles are larger than 100 nm due to aggregation. (Figure 2b) provides a breakdown of the size distribution for nanoparticles under 50 nm. Approximately 40% of these nanoparticles are smaller than 15 nm. Similar size distributions were obtained for CS-DTPA/TPP nanoparticles synthesized with a chitosan to DTPA weight ratio ranging from 1:2.5 to 1:25. Briefly, 44% - 73% of the nanoparticles are under 50 nm, and approximately 20% - 50% of these are smaller than 15 nm. Hence, they can reach the alveolar region in the deep lungs and achieve systemic drug delivery via blood circulation.

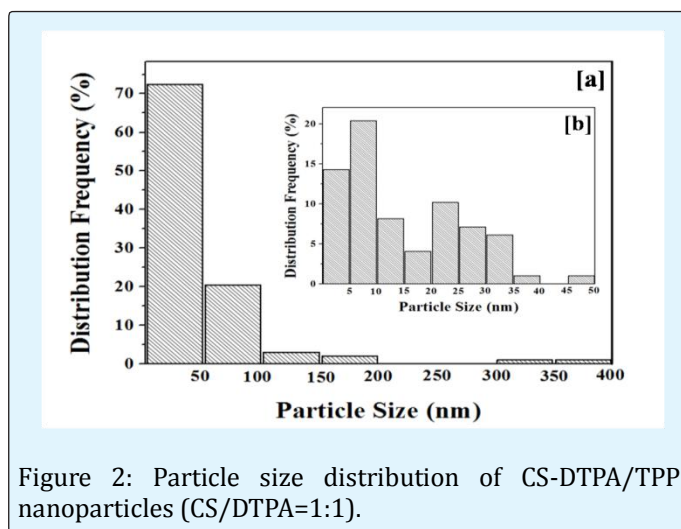


Figure 2: Particle size distribution of CS-DTPA/TPP nanoparticles (CS/DTPA=1:1).

Furthermore, FTIR was applied in analyzing the chemical structure of CS-DTPA/TPP dried powders to verify the chemical bond between chitosan and DTPA. In the preparation of CS-DTPA complex, an acidic aqueous medium protonated the $-NH_2$ functional group of Chitosan to form $-NH_3^+$ which then reacted with the $-COO^-$ functional group of DTPA-NaviaN-acetylation. The FTIR spectra of CS-DTPA/TPP dried powders synthesized with different chitosan to DTPA weight ratios are shown in Figure 3. Both O-H and C-H stretching vibrations appear in the range between 3700 and 2500 cm^{-1} . The $-CH_2-$ and $-CH-$ vibrations are found at 2939.3 and 2910.4 cm^{-1} . The peaks at 1633.6, 1571.9 and 1417.6 cm^{-1} correspond to the stretching vibration of C=O (amide I), bending vibration of N-H (amide II), and stretching vibration of C-N (amide III), respectively [24]. The existence of amide bond is hence verified, proving that chitosan has successfully encapsulated DTPA in the nanoparticles. By increasing the weight ratio of DTPA to chitosan, the amide peaks become stronger because more $-NH_2$ functional groups of chitosan react with the $-COOH$ functional groups of DTPA to form $-CONH-$. Moreover, two peaks at 1282.6 and 1207.4 cm^{-1} involve the stretching vibration of C-O. Last, the peaks at 1083.9 and 1020.3 cm^{-1} are assigned to mannitol [30].

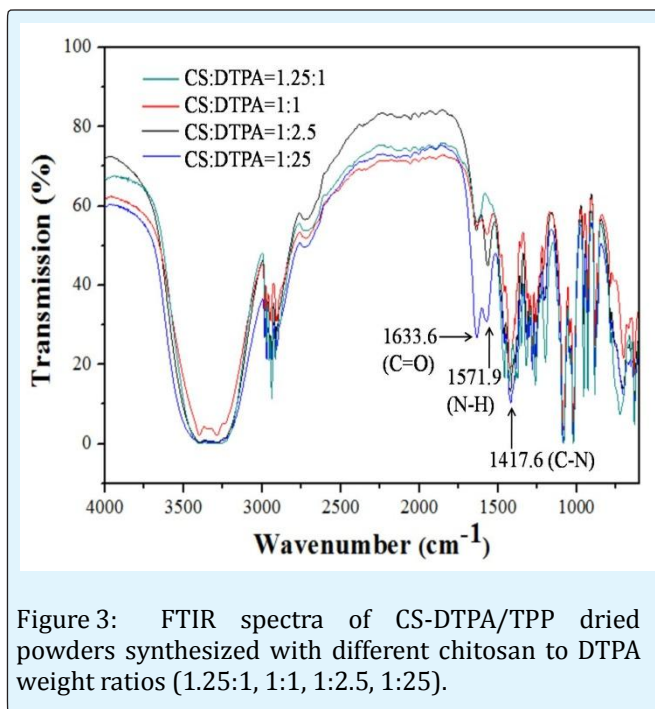


Figure 3: FTIR spectra of CS-DTPA/TPP dried powders synthesized with different chitosan to DTPA weight ratios (1.25:1, 1:1, 1:2.5, 1:25).

***In vitro* Release of DTPA from CS-DTPA/TPP nanoparticles**

In vitro release of DTPA from CS-DTPA/TPP nanoparticles was conducted in the simulated lung fluid (pH 7.4) at 37°C to demonstrate the potential for extended decorporation of radio nuclides. After the CS-DTPA/TPP/mannitol dry powders were dispersed in the fluid, mannitol dissolved away quickly from the CS-DTPA/TPP nanoparticles. The encapsulated DTPA could then be released continuously over a period of many hours. The concentration of DTPA in dialysate samples were determined by LC-MS/MS analysis with reference to a standard calibration curve. However, DTPA is a chelating agent that can form stable complexes with various metal ions such as Ca²⁺, Cd²⁺, Co²⁺, Cu²⁺, Mn²⁺ and Zn²⁺ [31]. The formation of multiple metal complexes was a challenge for LC-MS/MS determination of DTPA. It was

necessary to convert DTPA to a single metal complex. Formation constants for metal-DTPA complexes are in the order of Fe³⁺> Cu²⁺> Al³⁺> Zn²⁺ [32]. Among these essential metals, Fe³⁺ has the highest binding affinity with DTPA [33]. Specifically, the complex formation constants are 28.6 and 21.5 for Fe³⁺-DTPA and Cu²⁺-DTPA. Therefore, Fe³⁺ was added into all DTPA standard solutions and dialysate samples before LC-MS/MS analysis. This prevented the formation of DTPA complexes with other metal ions existing in the simulated lung fluid, thus improving the accuracy of released DTPA determination by LC-MS/MS. Figure 4a shows an example of a liquid chromatogram for DTPA and Figure 4b shows the standard calibration curve that was constructed from the peak areas of Fe³⁺-DTPA in the chromatograms obtained for a series of DTPA standard solutions by LC-MS/MS analysis at m/z=445.

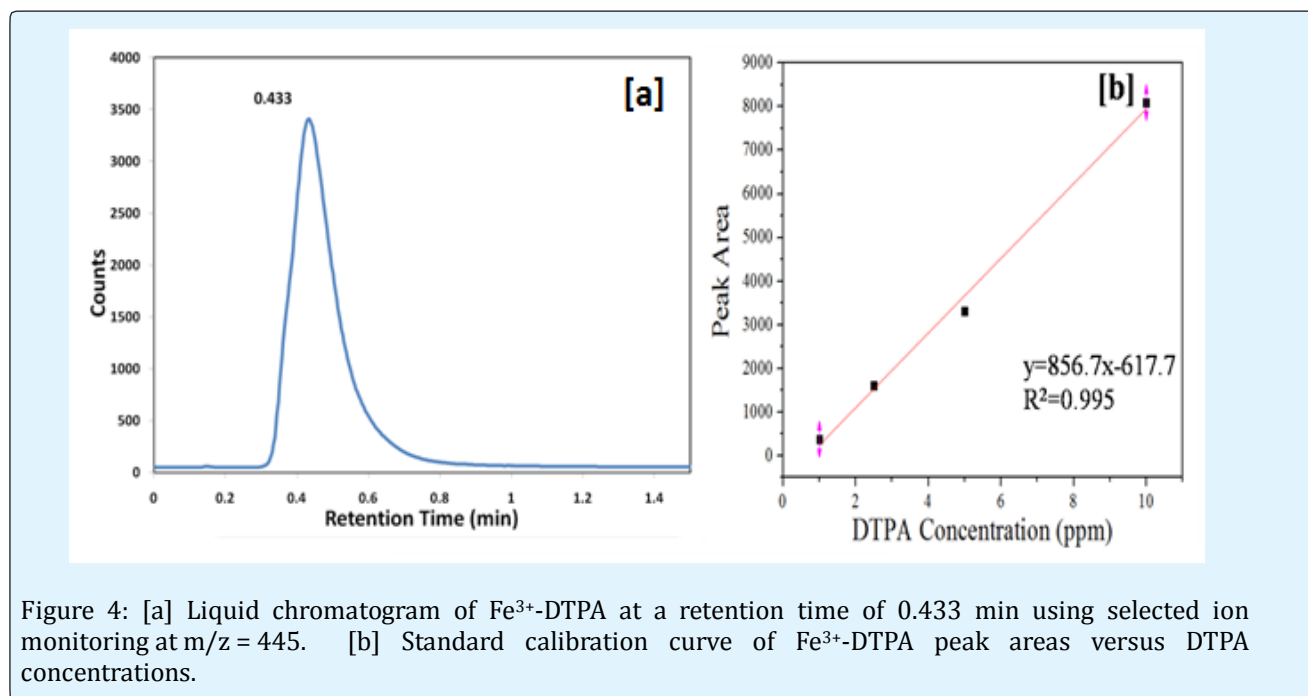


Figure 4: [a] Liquid chromatogram of Fe³⁺-DTPA at a retention time of 0.433 min using selected ion monitoring at m/z = 445. [b] Standard calibration curve of Fe³⁺-DTPA peak areas versus DTPA concentrations.

Based on the linear trend line equation, the concentration of DTPA (C_i) in each unknown dialysate sample i could be calculated. The cumulative amount of DTPA released (A_n) was then calculated using the following equation:

$$A_n = V_e \sum_{i=1}^{n-1} C_i + V_0 C_n$$

Where V_e is the volume of each dialysate sample (3mL), V_0 is the volume of simulated lung fluid outside the

dialysis tube (50mL), and C_n represents the concentration of DTPA in the nth sample.

In vitro release of DTPA from the CS-DTPA/TPP nanoparticles was conducted in the simulated lung fluid without adding lysozyme. The cumulative amounts of DTPA released from CS-DTPA/TPP nanoparticles with different chitosan to DTPA weight ratios are shown in Figure 5.

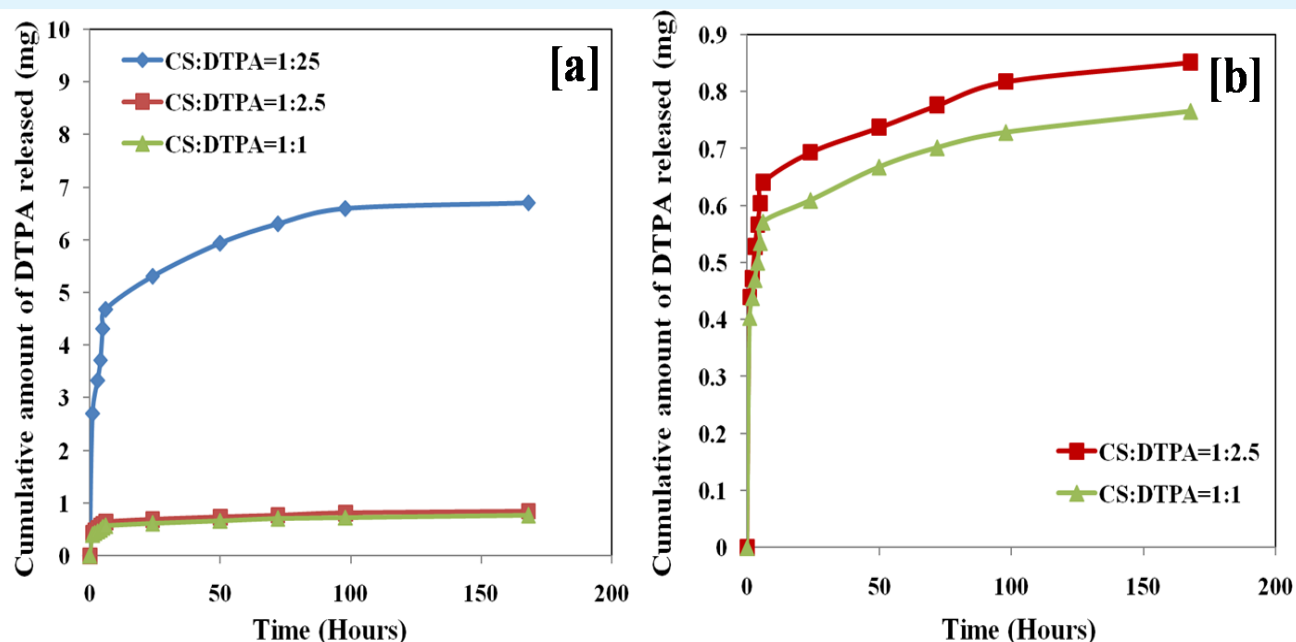


Figure 5: [a] Cumulative amount of DTPA released from CS-DTPA/TPP nanoparticles in simulated lung fluid without adding lysozyme; [b] Magnified DTPA release profiles for CS/DTPA=1:2.5 and CS/DTPA=1:1.

For all of the CS-DTPA/TPP nanoparticles (CS/DTPA = 1:1, 1:2.5 and 1:25) prepared in this work, the release profiles exhibit an initial burst, a slow release in the next stage and a relatively stable level in the final stage. In the initial 6 hours, the cumulative amounts of DTPA released (from 50 mg of dry powders containing 9.5 mg of DTPA) rapidly reach 0.57, 0.64 and 4.7mg, respectively. In the next 92 hours, the cumulative DTPA amounts slowly increase to 0.73, 0.82 and 6.6mg, respectively. After 98 h, there is no significant increase in the cumulative DTPA amounts. After 168 hours (7 days), the final cumulative amounts of DTPA are 0.77, 0.85 and 6.7 mg, respectively. Hence, initially the CS-DTPA/TPP nanoparticles have gradually released 70-75% of the final cumulative DTPA amount over an extended period of 6 hours. This represents a significant improvement compared with the conventional administration of DTPA directly into the lung fluid.

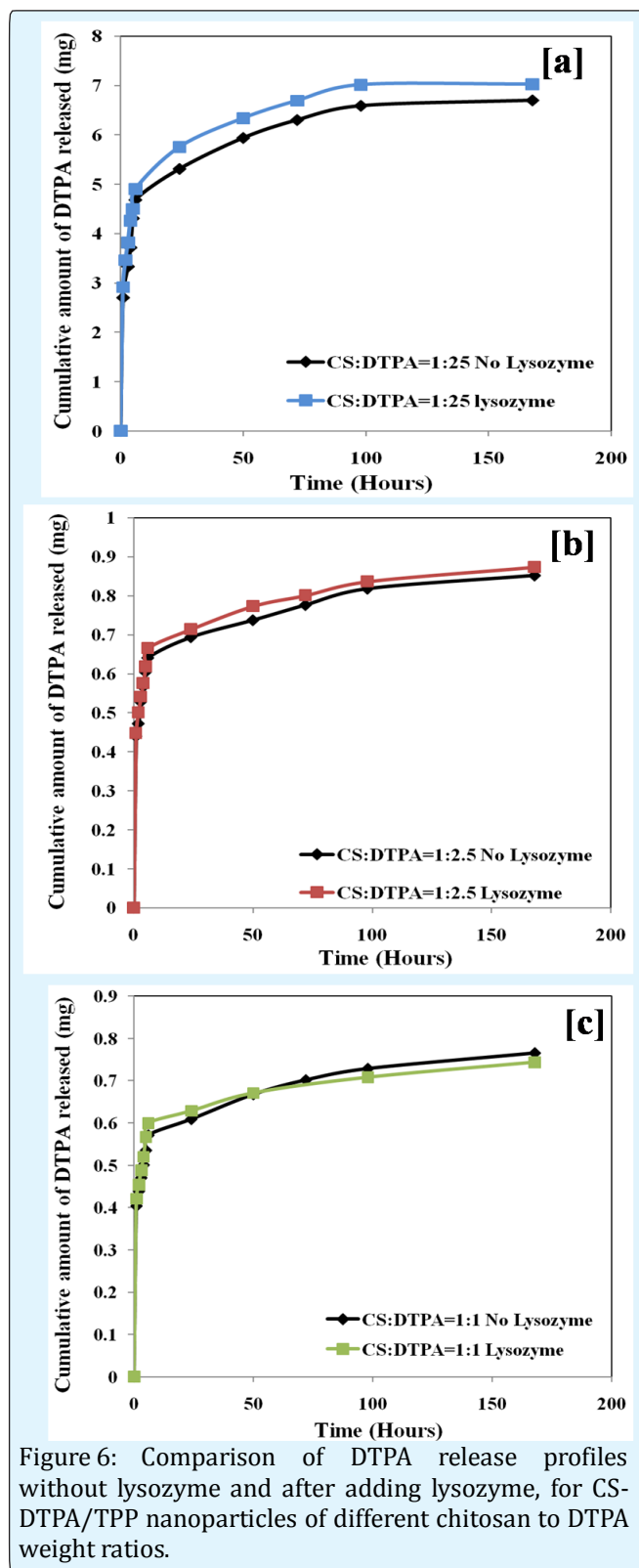
Effect of lysozyme on DTPA release profiles

Based on the literature, the drug carrier chitosan is a biodegradable polymer and its chain structure can be decomposed by lysozyme which is an enzyme existing *in vivo* [24]. Could this have a negative impact on the extended DTPA release profiles? *In vitro* release testing was next conducted in the simulated lung fluid after adding lysozyme. The cumulative amounts of DTPA

released from CS-DTPA/TPP nanoparticles in the simulated lung fluid after adding lysozyme are shown in Figure 6, for comparison with those obtained without lysozyme. Apparently the presence of lysozyme does not significantly change the cumulative amount of DTPA released from the CS-DTPA/TPP nanoparticles. After 168 hours (7 days), the cumulative amounts of DTPA released from CS-DTPA/TPP nanoparticles of the highest weight ratio (DTPA/CS=25:1) are 7.03 mg after adding lysozyme and 6.70 mg without lysozyme. The final cumulative amounts of DTPA released from CS-DTPA/TPP nanoparticles of a medium weight ratio (DTPA/CS=2.5:1) reach 0.87mg and 0.85mg, respectively. Similarly, the final cumulative amounts of DTPA released from CS-DTPA/TPP nanoparticles of the lowest weight ratio (DTPA/CS=1:1) are 0.74 mg and 0.77 mg.

DTPA release mechanism

Agnihotri et al. [28] have previously pointed out that many factors, such as the density, extent of cross-linking, morphology and size of the particles, physicochemical properties of the drug, as well as the presence of adjuvants, can affect the time profile of drug release from chitosan-based particles. Furthermore, *in vitro* release can also be affected by the pH, ionic strength, and presence of enzymes in the release medium.



Three different mechanisms maybe involved in drug release from chitosan-based particles: (a) release from particle surface, (b) diffusion through the swollen matrix, and (c) polymer degradation resulting in the release. Generally, more than one mechanism is involved in any drug release system [34]. Chitosan is a hydrophilic polymer, so mainly mechanisms (a) and (b) could control the release of DTPA from the CS-DTPA/TPP nanoparticles studied in the present work. The simulated lung fluid probably penetrated the nanoparticles and resulted in swelling of the CS-DTPA-TPP matrix, thus facilitating DTPA diffusion out of the nanoparticles. Although the chain structure of chitosan were broken by lysozyme at the β -(1 \rightarrow 4) links, the TPP cross-linkers did not free up the CS-DTPA quickly to allow for rapid release of DTPA from the degrading CS-DTPA/TPP nanoparticles. By analogy, extended release of DTPA can reasonably be expected despite abundant lysozyme *in situ* when it comes to decorporation of internalized plutonium and americium.

Conclusions

The ionic gelation method has been successfully applied to the preparation of CS-DTPA/TPP nanoparticles, wherein TPP is the cross-linker that pulls the CS polymer together to form a spherical morphology with a gel-like matrix for extended release of the encapsulated decorporation agent DTPA. Most CS-DTPA/TPP nanoparticles are smaller than 50 nm, no matter what the DTPA to chitosan weight ratio is. N-acetylation has occurred between the -NH_2 functional groups of chitosan and the -COOH functional groups of DTPA. Initially the CS-DTPA/TPP nanoparticles gradually release 70-75% of the final cumulative DTPA amount over an extended period of 6 hours. This is potentially useful in delivering a controlled amount of decorporation agent into the blood stream through the lungs. After 98 hours, the cumulative amount reaches a steady-state level as dictated by chemical equilibrium (between the CS-DTPA complex and dissociated DTPA) and diffusion kinetics (as DTPA moves down a concentration gradient) through the swollen CS-TPP matrix for free release at the nanoparticle surface. Lysozyme, present in the lung fluid, has no negative impact on the extended release profile or final cumulative amount of DTPA. To better preserve the nanoparticles, freeze drying can be applied to produce dried powders using mannitol as a dispersant to suppress the aggregation of nanoparticles. The dried powders are easy for accurate dosing into deployable medication devices such as a personal inhaler.

Acknowledgements

Partial funding by the Natural Sciences and Engineering Research Council and facility support by Health Canada are gratefully acknowledged.

References

- List of nuclear power accidents by country (2016) Retrieved from https://en.wikipedia.org/wiki/List_of_nuclear_power_accidents_by_country#Canada.
- Devell L, Tovedal H, Bergström U, Appelgren A, Chyssler J, et al. (1986) Initial observations of fallout from the reactor accident at Chernobyl. *Nature* 321: 192-193.
- Kinoshita N, Sueki K, Sasa K, Kitagawa J, Ikarashi S, et al. (2011) Assessment of individual radionuclide distributions from the Fukushima nuclear accident covering central-east Japan. *PNAS* 108(49): 19526-19529.
- Ansoborlo É, Prat O, Moisy P, Den Auwer C, Guilbaud P, et al. (2006) Actinide speciation in relation to biological processes. *Biochimie* 88(11): 1605-1618.
- Ansoborlo É, Amekraz B, Moulin C, Moulin V, Taran F, et al. (2007) Review of actinide decorporation with chelating agents. *Comptes Rendus Chimie* 10(10-11): 1010-1019.
- Fisher DR (2000) Decorporation: officially a word. *Health Physics* 78(5): 563-565.
- Wood R, Sharp C, Gourmelon P, Le Guen B, Stradling GN, et al. (2000) Decorporation treatment-medical overview. *Radiation Protection Dosimetry* 87(1): 51-56.
- US Department of Health and Human Services-Project bioshield annual report to congress – August 2007 through December 2008.
- Breustedt B, Blanchardon E, Berard P, Fritsch P, Giussani A, et al. (2009) Biokinetic modelling of DTPA decorporation therapy: the CONRAD approach. *Radiation Protection Dosimetry* 134(1): 38-48.
- Grémy O, Laurent D, Coudert S, Griffiths NM, Miccoli L (2016) Decorporation of Pu/Am actinides by chelation therapy: new arguments in favor of an intracellular component of DTPA action. *Radiation Research* 185(6): 568-579.
- Bonin L, Aupiais J, Kerba M, Moisy P, Topin S, et al. (2016) Revisiting actinide-DTPA complexes in aqueous solution by CE-ICPMS and *ab initio* molecular dynamics. *RSC Adv* 6(67): 62729-62741.
- Huckle JE, Sadgrove MP, Leed MG, Yang YT, Mumper RJ, et al. (2016) Synthesis and physicochemical characterization of a diethyl ester prodrug of DTPA and its investigation as an oral decorporation agent in rats. *AAPS J* 18(4): 972-980.
- Marcus CS (2004) Administration of decorporation drugs to treat internal radionuclide contamination: medical emergency response to radiologic incidents. *RSO Magazine* 9: 9-15.
- Ménétrier F, Grappin L, Raynaud P, Courtay C, Wood R, et al. (2005) Treatment of accidental intakes of plutonium and americium: guidance notes. *Applied Radiation and Isotopes* 62(6): 829-846.
- National Council on Radiation Protection and Measurements (2008) Management of persons contaminated with radionuclides: handbook.
- Phan G, Herbet A, Cholet S, Benech H, Deverre JR, et al. (2005) Pharmacokinetics of DTPA entrapped in conventional and long-circulating liposomes of different size for plutonium decorporation. *J Control Release* 110(1): 177-188.
- Gervelas C, Serandour AL, Geiger S, Grillon G, Fritsch P, et al. (2007) Direct lung delivery of a dry powder formulation of DTPA with improved aerosolization properties: effect on lung and systemic decorporation of plutonium. *J Control Release* 118(1): 78-86.
- Kurita K (2006) Chitin and chitosan: functional biopolymers from marine crustaceans. *Marine Biotechnology* 8(3): 203-226.
- Rinaudo M (2006) Chitin and chitosan: properties and applications. *Progress in Polymer Science* 31(7): 603-632.
- Aksungur P, Sungur A, Ünal S, Iskit AB, Squier CA, et al. (2004) Chitosan delivery systems for the treatment of oral mucositis: *in vitro* and *in vivo* studies. *J Control Release* 98(2): 269-279.

21. He P, Davis SS, Illum L (1998) *In vitro* evaluation of the mucoadhesive properties of chitosan microspheres. *International Journal of Pharmaceutics* 166(1): 75-88.
22. Aspden TJ, Illum L, Skaugrud Ø (1996) Chitosan as a nasal delivery system: evaluation of insulin absorption enhancement and effect on nasal membrane integrity using rat models. *European Journal of Pharmaceutical Sciences* 4(1): 23-31.
23. Wang L, Cui F, Gao P (2004) Progress in research of chitosan and its derivatives in pharmaceutical aspect. *Chinese Journal of New Drugs* 2004: 212-215.
24. Vimal S, Majeed SA, Taju G, Nambi KSN, Raj NS, et al. (2013) Chitosan tripolyphosphate (CS/TPP) nanoparticles: preparation, characterization and application for gene delivery in shrimp. *Acta Trop* 128(3): 486-493.
25. Zainol I, Ghani SM, Mastor A, Derman MA, Yahya MF (2009) Enzymatic degradation study of porous chitosan membrane. *Materials Research Innovations* 13(3): 316-319.
26. Ren D, Yi H, Wang W, Ma X (2005) The enzymatic degradation and swelling properties of chitosan matrices with different degrees of N-acetylation. *Carbohydr Res* 340(15): 2403-2410.
27. Liu Y, Zhou X, Wan J, Hu D, Zhang Y (2012) Study on radiation protection of WSC-DTPA nanoparticles. *Journal of Radiation Research and Radiation Processing* 30(5): 309-315.
28. Agnihotri SA, Mallikarjuna NN, Aminabhavi TM (2004) Recent advances on chitosan-based micro-and nanoparticles in drug delivery. *J Control Release* 100(1): 5-28.
29. Marques MRC, Loebenberg R, Almukainzi M (2011) Simulated biological fluids with possible application in dissolution testing. *Dissolution Technologies* 18: 15-28.
30. Burger A, Henck J, Hetz S, Rollinger JM, Weissnicht AA, et al. (2000) Energy/temperature diagram and compression behavior of the polymorphs of d-mannitol. *J Pharm Sci* 89(4): 457-468.
31. Zhou S, Zhang B, Sturm E, Teagarden DL, Schöneich C, et al. (2010) Comparative evaluation of disodium edetate and diethylenetriaminepentaacetic acid as iron chelators to prevent metal -catalyzed destabilization of a therapeutic monoclonal antibody. *J Pharm Sci* 99(10): 4239-4250.
32. Kontoghiorghe C, Kolnagou A, Kontoghiorghes G (2015) Phytochelators intended for clinical use in iron overload, other diseases of iron imbalance and free radical pathology. *Molecules* 20(11): 20841-20872.
33. Miller S, Wang X, Bowman B (2010) Pharmacological properties of orally available, amphipathic polyaminocarboxylic acid chelators for actinide decorporation. *Health Physics* 99(3): 408-412.
34. Courrier HM, Butz N, Vandamme TF (2002) Pulmonary drug delivery systems: recent developments and prospects. *Crit Rev Ther Drug Carrier Syst* 19(4-5): 425-498.